Original Article
Long-term effect of extracorporeal shock wave therapy on attenuating radiation-induced chronic cystitis in rat

Yen-Ta Chen[1,2], Chih-Chao Yang[3], Pei-Hsun Sung[4,5], Kun-Chen Lin[6], John Y Chiang[7,8], Chi-Ruei Huang[4,5], Kuan-Hui Huang[9], Fei-Chi Chuang[9], Yi-Ching Chu[4,5], Eng-Yen Huang[10,11], Hon-Kan Yip[4,5,12,13,14]

[1]Division of Urology, Department of Surgery, Kaohsiung Chang Gung Memorial Hospital, College of Medicine, Chang Gung University, Kaohsiung, Taiwan; [2]Center for Shockwave Medicine and Tissue Engineering, Kaohsiung Chang Gung Memorial Hospital, Kaohsiung, Taiwan; [3]Division of Nephrology, Department of Internal Medicine, Kaohsiung Chang Gung Memorial Hospital, College of Medicine, Chang Gung University, Kaohsiung, Taiwan; [4]Division of Cardiology, Department of Internal Medicine, Kaohsiung Chang Gung Memorial Hospital and Chang Gung University College of Medicine, Kaohsiung, Taiwan; [5]Center for Shockwave Medicine and Tissue Engineering, Kaohsiung Chang Gung Memorial Hospital, Kaohsiung, Taiwan; [6]Department of Anesthesiology, Kaohsiung Chang Gung Memorial Hospital, Chang Gung University College of Medicine, Kaohsiung, Taiwan; [7]Department of Computer Science and Engineering, National Sun Yat-sen University, Kaohsiung, Taiwan; [8]Department of Healthcare Administration and Medical Informatics, Kaohsiung Medical University, Kaohsiung, Taiwan; [9]Department of Obstetrics and Gynecology, Kaohsiung Chang Gung Memorial Hospital, College of Medicine, Chang Gung University, Kaohsiung, Taiwan; [10]Department of Radiation Oncology, Kaohsiung Chang Gung Memorial Hospital, College of Medicine, Chang Gung University, Kaohsiung, Taiwan; [11]School of Traditional Chinese Medicine, Chang Gung University College of Medicine, Taoyuan, Taiwan; [12]Institute for Translational Research in Biomedicine, Kaohsiung Chang Gung Memorial Hospital, Kaohsiung, Taiwan; [13]Department of Medical Research, China Medical University Hospital, China Medical University, Taichung, Taiwan; [14]Department of Nursing, Asia University, Taichung, Taiwan

Abstract: Background: This study tested the long-term effect of extracorporeal shock wave (ECSW) therapy on ameliorating radiotherapy-induced chronic cystitis (CC) in rat. Methods and results: Adult-female SD rats (n = 24) were equally categorized into group 1 (normal control), group 2 (CC induced by radiotherapy with 450 cGy twice with a four-hour interval to the urinary bladder), group 3 [CC with ECSW treatment (0.1 mJ/mm^2/120 impulses once every 3 days after radiotherapy)]. Bladder specimens were harvested by day 60 after radiotherapy. By day 60, the degree of detrusor contraction was significantly reduced in group 2 than groups 1 and 3, and significantly reduced in group 3 than in group 1 (P < 0.0001). Number of WBC, occulted blood and bacteria were significantly higher in group 2 than in groups 1 and 3 (P < 0.01), but they showed no difference between the latter two groups (P > 0.3). The protein expressions of oxidative stress (NOX-1/NOX-2/oxidized protein), apoptosis (cleaved-caspase-3/cleaved-PARP), DNA-damaged marker (γ-H2AX), fibrosis (TGF-β/Smad3) and inflammatory signaling (TLR-4/MYD88/Mal/TRAF6/p-IκBα/p-NFκB/TNF-α/MMP-9/COX-2) were significantly higher in group 2 than in group 1, and were significantly reduced in group 3 (all P < 0.001). The cellular expressions of inflammatory (CD14+/CD68+/MIF+/MMP-9), immunoreactive (CD4+/CD8+) and cytokeratin (CK17/CK18) biomarkers, and collagen-deposition/fibrotic areas as well as bladder-damaged score/disruption of the bladder mucosa displayed an identical pattern compared to that of oxidative stress among the three groups (all P < 0.0001). Conclusion: The long-term effect of ECSW treatment was reliable on protecting the urinary bladder from radiation-induced CC.

Keywords: Radiation, chronic cystitis, inflammation, urinary bladder contractility

Introduction

Despite state-of-the-art advances in chemotherapy, hormone therapy and target therapy as well as immunotherapy for advanced cancers, radiotherapy still plays an essential role on palliative therapy for advanced stage of some solid cancers such as brain tumor, lung cancers and urogenital/gynecologic cancers [1-5]. However, a fly in the ointment is that radiotherapy has been found to commonly induce hemorrhagic cystitis (HC), gross hematuria and

late radiation-induced chronic cystitis (CC), which not merely hinder the patient's quality of life and social activity but also induce psychiatric issues, urinary tract infection/sepsis, obstructive uropathy and renal failure as well as increase the risk of mortality [6-10].

During the last decades, plentiful modalities, including pharmacological agents, surgical interventions and even hyperbaric oxygen therapy, have been extensively applied for the HC [11-18]. However, their efficacies are contradictory, highlighting that treatment of radiotherapy-induced HC/CC and the associated complications remains a formidable challenge. Accordingly, a safe and efficacious treatment alternative is still eagerly awaited.

In view of pathophysiology of radiation cystitis that is mainly caused by activation of an inflammatory cascade leading to tissue swelling, mucosa damage, necrosis, and smooth muscle destruction and finally fibrosis [19-22], eradication of the inflammatory reactions may prove as an innovative therapeutic strategies for those of HC/CC patients refractory to conventional treatment.

Previous studies have established that extracorporeal shock wave (ECSW) therapy is able to inhibit the inflammatory reaction and oxidative stress, and augment the angiogenesis [23, 24]. Besides, our studies have displayed that ECSW therapy is not only safe, but has capacities of pro-angiogenesis, anti-ischemia, anti-fibrosis, anti-inflammation, and pain-alleviating effects [25-29]. Based on these aforementioned issues [19-29], we have recently performed a study with a period of 28 days to address the impact of ECSW on reducing the radiation-induced HC/CC in rodent [30]. Our results are attractive and promising. However, this study also has limitations, such as the optimal dosage of radiation and long-term effect of ECSW therapy with appropriate energy on radiation-induced HC were regrettably left unaddressed. Accordingly, this study was designed to answer the limitations of our recent study [30].

Materials and methods

Ethics and animal care

All animal procedures were approved by the Institute of Animal Care and Use Committee at Kaohsiung Chang Gung Memorial Hospital (Affidavit of Approval of Animal Use Protocol No. 2016012804) and performed in accordance with the Guide for the Care and Use of Laboratory Animals.

Animals were housed in an Association for Assessment and Accreditation of Laboratory Animal Care International (AAALAC; Frederick, MD, USA)-approved animal facility in our hospital with controlled temperature and light cycles (24°C and 12/12 light cycle).

Rationale of ECSW energy utilized in the present study

The purpose of this study was to evaluate the long-term effect of ECSW on protecting the urinary bladder against the radiotherapy. Thus, the study period was designed as a duration of 60 days after radiotherapy. Another evaluation was that ECSW application should resemble the clinical setting of "regularly intermittent administration" of the medicine for a chronic disease. Along this line of thinking, regularly intermittent application of ECSW to the urinary bladder was performed for the animals. Based on these considerations, the safety of ECSW had to be considered, especially when regular and consistent application of ECSW was utilized in the present study. According to our previous in vitro [31] and in vivo [23, 25-30] studies, we found that the safest and lowest energy of ECSW with promising efficacy was 0.1 mJ/mm^2/120 impulses. This was the reason why we utilized the "0.1 mJ/mm^2/120 impulses once every 3 days after radiation" (i.e., a total of 20 times in the present study).

Rationale of radiotherapy dosage (refer to Figure 1) and duration of study period

Practically, for achieving greatest efficacy, the dosage of radiotherapy for solid cancers of urogenital/gynecologic origin is always quite high in order to kill the cancer cells that could explain why a lot of side effects are frequently encountered in those urogenital/gynecologic patients after receiving this therapy [19-22]. On the other hand, for safety, the dosage of radiotherapy in our previous animal model study [30] was designed as low dosage (i.e., 300 cGy). This, therefore, raises the question that the results of our animal model of study [30] might not truthfully reflect the daily clinical practice. Accordingly, in the present study, except the low dose of our previous study (i.e., 300 cGy twice with a four-hour interval to the urinary bladder of one animal), we performed a pilot
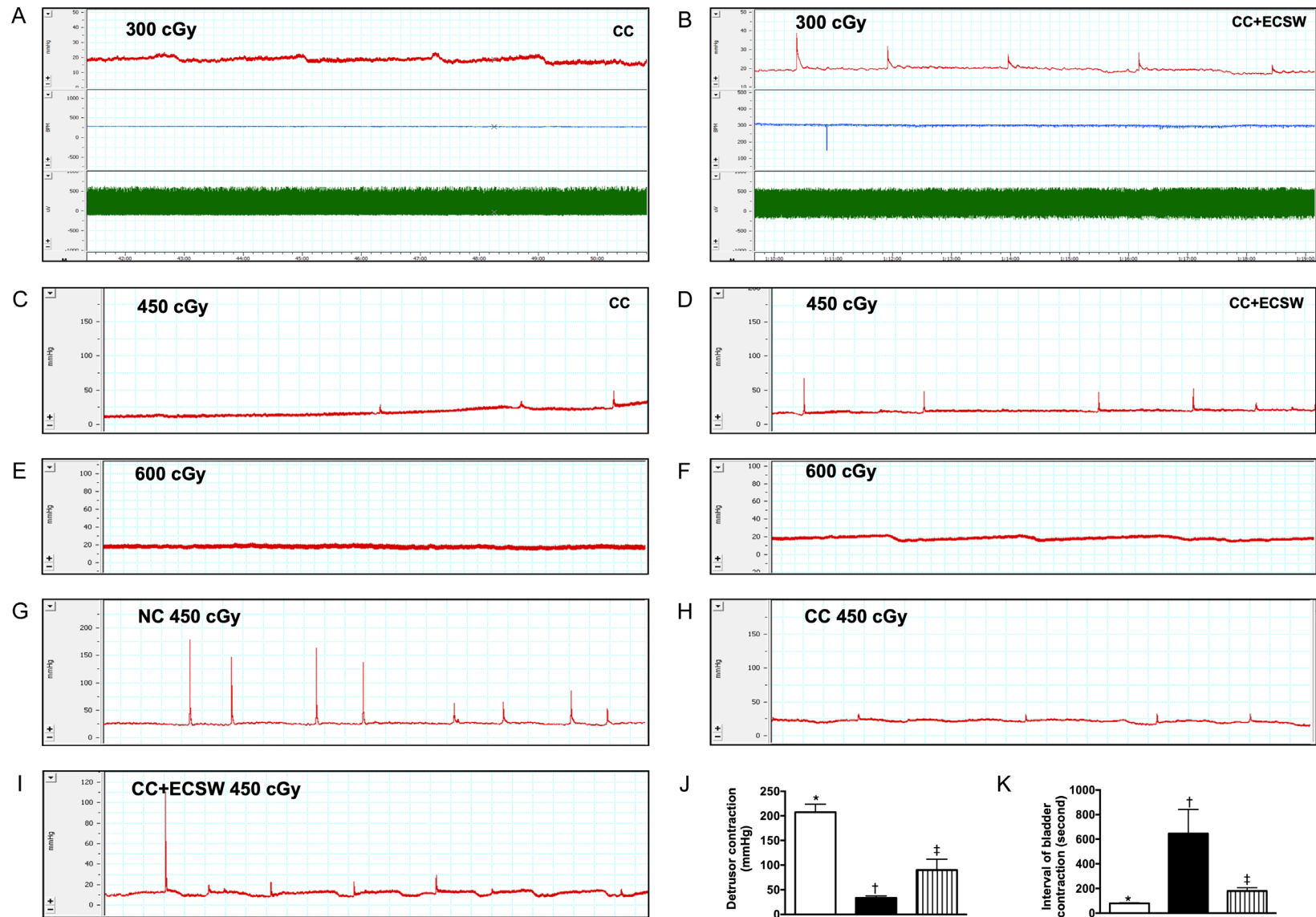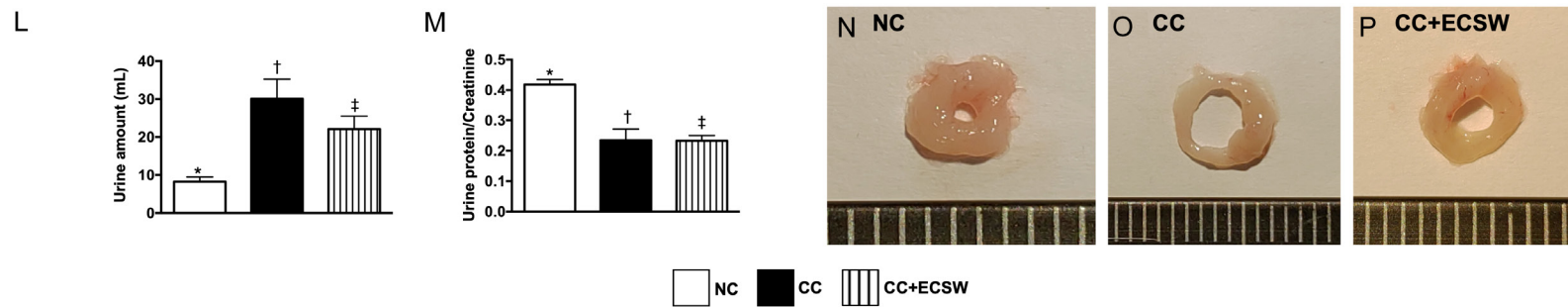
Figure 1. Pilot study, urodynamic study of bladder contraction, urine amount and ratio of urine protein to urine creatinine at day 60 after radiotherapy. (A-F) Escalation of dosage of radiation energy (i.e., stepwise increase of the radiotherapy dosage) in the pilot study with consistent ECSW application (i.e., 0.1 mJ/mm^2/120 impulses/once every 3 days after radiation). We utilized 300 cGy (A, B), 450 cGy (C, D) and 600 cGy (E, F)/twice with 4-h interval for each animal in CC (A, C, E) and CC + ECSW (B, D, F) groups (n = 2/each group). By day 60 after CC induction, the results showed that no detrusor contractility wave was observed in either CC only or in CC + ECSW animals in 600 cGy, only CC + ECSW animals had notable detrusor contractility wave in 450 cGy and 300 cGy. Thus, radiotherapy for induction of CC by 450 cGy twice with 4-h interval was utilized for this study. (G-I) Illustrating the anatomical structure of urinary bladder in three groups. As compared with NC (G), the wall of urinary bladder was notably thinner and the lumen of urinary bladder was more increased in CC animals (H), suggesting that the elastic property of urinary bladder was diminished in CC animals. However, these phenomena were reversed in CC animals after receiving ECSW treatment (I). (J-L) Illustrating the graphics of urinary bladder contractility. (M) Analytical result of detrusor contraction, * vs. other groups with different symbols (†, ‡), P < 0.0001. (N) Interval of bladder contraction, * vs. other groups with different symbols (†, ‡), P < 0.0001. (O) Urine amount (ml) at day 60, * vs. other groups with different symbols (†, ‡), P < 0.001. (P) Ratio of urine protein to creatinine, * vs. †, P < 0.001. All statistical analyses were performed by one-way ANOVA, followed by Bonferroni multiple comparison post hoc test (n = 6 for each group). Symbols (*, †, ‡) indicate significance at the 0.05 level. NC = normal control; CC = chronic cystitis; ECSW = extracorporeal shock wave.

study to test the safety of two different doses, i.e., (1) moderate dose of radiation (450 cGy twice with a four-hour interval) and (2) high dose of radiation (600 cGy twice with a four-hour interval), suggesting that this was a scientific escalation of radiotherapy dosage. Our results showed that the urodynamic study by day 60 after CC induction showed no detrusor contraction activity in with and without ECSW therapy on highest dose of radiotherapy (i.e., 600 cGy) (ref. to **Figure 1**). However, the detrusor contraction of HC animals was significantly preserved in with than in without ECSW therapy in moderate dose of radiotherapy (i.e., 450 cGy) (ref. to **Figure 1**). Thus, this dose of radiotherapy was utilized in the present study.

The study period of our previous study [30] was only 28 days, which raises the question whether the long-term impact of ECSW on reducing the HC/CC caused by radiation would be also effective. Accordingly, the study period of this study, specifically designed to respond to this question, was extended to 60 days.

Animal model of chronic cystitis, animal grouping, and energy of ECSW

The procedure and protocol have been described in our resent report [30]. In detail, the pathogen-free, adult male Sprague-Dawley (SD) rats (n = 24) weighing 300-325 g (Charles River Technology, BioLASCO Taiwan, Taiwan) were randomized and equally divided into normal control (NC) group, chronic cystitis (CC) group [induced by radiation to simulate brachytherapy (450 cGy twice) to the bladder surface over the skin at a time interval of 4 h], and CC + ECSW group (0.1 mJ/mm^2/120 impulses/one time/per 3-day time-interval after radiotherapy). ECSW was applied to the skin surface above the urinary bladder at different time points of treatment. During the procedures, all animals were anesthetized by inhalation of 2.0% isoflurane, and placed in a supine position on a warming pad at 37°C for radiation/ECSW.

Eight animals in each group were utilized for urodynamic study. On the other hand, six animals in each group were used for molecular-cellular studies.

Procedure and protocol of urodynamic test (bladder pressure assessment)

The procedure of intravesical pressure measurement was in accordance to the previous report [30]. After being anesthetized with 2.0% inhalational isoflurane, the rat was placed in supine position on a heating pad maintained at 37°C. A polyethylene catheter (PE50, Clay Adams, NJ, USA), which was inserted through the urethra into the urinary bladder, was connected to a pressure transducer (BP Transducer Model MLT0380, Ad Instruments, NSW, Australia) and syringe pump (Microinjection pump Model KDS100, KD Scientific Inc., MA, USA) that delivered normal saline to the urinary bladder at a rate of 0.05 mL/min. Intravesical pressure signals, recorded continuously for 90 minutes, were converted real-time into electrical signals (PowerLab 16/35 Model PL3516, Ad Instruments, NSW, Australia) and amplified (Bridge Amp Model FE221, and Animal Bio Amp Model: FE136, Ad Instruments, NSW, Australia) before being stored in a computer for later analysis (PowerLab 16/35 Model PL3516, Ad Instruments, NSW, Australia).

24-h urine collection for amount and the ratio of urine protein to urine creatinine by day 60, and sporadic urine collection for examination at days 0, 28 and 60 after CC induction

The procedure and protocol have been described in our previous reports [23, 30]. In detail, sporadic urine was collected in all animals at days 0, 28 and 60 after CC induction to determine relevant pathological parameters.

For the collection of 24-hr urine to assess urine amount and the ratio of urine protein to urine creatinine, each animal was put in a metabolic cage (DXL-D, space: 190 × 290 × 550 mm^3, Suzhou Fengshi Laboratory Animal Equipment Co. Ltd., China) for 24 hours with free access to food and water.

Immunohistochemical and immunofluorescent studies

The procedures and protocols for immunohistochemistry (IHC) and immunofluorescence (IF) examinations were as previously described (24, 26-33). In detail, for IHC staining, rehydrated paraffin sections were first treated with 3% H$_2$O$_2$ for 30 minutes and incubated with Immuno-Block reagent (BioSB) for 30 minutes

Table 1. Semi-quantitative results of sporadic urine-routine examinations at days 0, 28 and 60 among the three groups

Variables	SC	CC	CC + ECSW	p-value*
At day 0				
Occulted blood	negative	negative	negative	-
Proteinuria	negative	negative	negative	-
Urine glucose	negative	negative	negative	-
Nitrite	negative	negative	negative	-
Leukocyte	negative	negative	negative	-
Red blood cell	0-1	0-1	0-1	-
White blood cell	0-1	0-1	0-1	-
Bacteria	none	none	none	-
Cast formation	none	none	none	-
At day 28				
Occulted blood	negative	+ to ++	negative	<0.05
Proteinuria	negative	+	negative	>0.1
Urine glucose	negative	negative	negative	-
Nitrite	negative	positive	positive	<0.05
Leukocyte	negative	2+	negative	<0.001
Red blood cell	0-1	0-2	0-1	-
White blood cell	0-1	2-5	0-1	<0.001
Bacteria	none	3+	2+	<0.001
Cast formation	none	none	none	-
At day 60				
Occulted blood	negative	trace	trace	-
Proteinuria	negative	+	negative	>0.1
Urine glucose	negative	negative	negative	-
Nitrite	negative	positive	negative	<0.05
Leukocyte	negative	+	negative	<0.05
Red blood cell	0-1	0-1	0-1	-
White blood cell	0-1	2-5	0-1	<0.001
Bacteria	none	3+	1+	<0.001
Cast formation	none	none	none	-

Data are expressed as mean + SD. SC = sham control; CC = chronic cystitis; ECSW = extracorporeal shock wave. *indicate n = 6 for each group per each time interval.

trols. Three sections of bladder specimens were analyzed in each rat. For quantification, three randomly selected high-power fields (HPFs, 200 × for IHC and IF studies) were analyzed in each section. The percentage of positively-stained cells per high-power field (HPF) for each animal was then determined. To analyze the integrity of collagen synthesis and deposition, three bladder paraffin sections (4 μm) were stained with picro-Sirius red (1% Sirius red in saturated picric acid solution) for one hour at room temperature using standard methods. The integrated area (μm^2) of fibrosis in each section was calculated using Image Tool 3 (IT3) image analysis software (Health Science Center, University of Texas, San Antonio, USA). Three selected sections were quantified for each animal. Three randomly selected HPFs (100 ×) were analyzed in each section. After determining the number of pixel in each fibrotic area per HPF, the numbers of pixels obtained from the three HPFs were summed. The procedure was repeated in two other sections for each animal. The mean pixel number per HPF for each animal was then determined by summing all pixel numbers and divided by 9. The mean integrated area (μm^2) of fibrosis in quadriceps per HPF was obtained using a conversion factor of 19.24 (1 μm^2 corresponded to 19.24 pixels).

at room temperature. Sections were then incubated with primary antibodies specifically against CK17 (1:50, Abcam), CK18 (1:100, Abcam), CD4 (1:400, Gene Tex), CD8 (1:200, Bio-Rad), glycosaminoglycan (GAG) (ScyTek) and matrix metalloproteinase (MMP)-9 at 4°C overnight. Irrelevant antibodies and mouse control IgG were used as controls. IF staining was performed for the examination of CD14 (1:200, Proteintech), CD68 (1:100 Abcam) and macrophage migration inhibitory factor (MIF) (1:100, Abcam) using appropriate primary antibodies; irrelevant antibodies were used as con-

Histopathology scoring for the injury of epithelial layer in urinary bladder specimens from all animals was determined microscopically based on the results of Alcian Blue staining [i.e., for distributive intensity of glycosaminoglycan (GAG)] over the epithelial layer of urinary bladder according to manufacturer's instruction. The grading of epithelial injury and the formation of vacuoles (i.e., perinuclear cytoplasmic vacuolization) as well as cytokeratin formation in the epithelial layer in 10 randomly chosen, non-overlapping fields (100 ×) for each animal was as follows: 0 (none), 1 (≤ 10%), 2
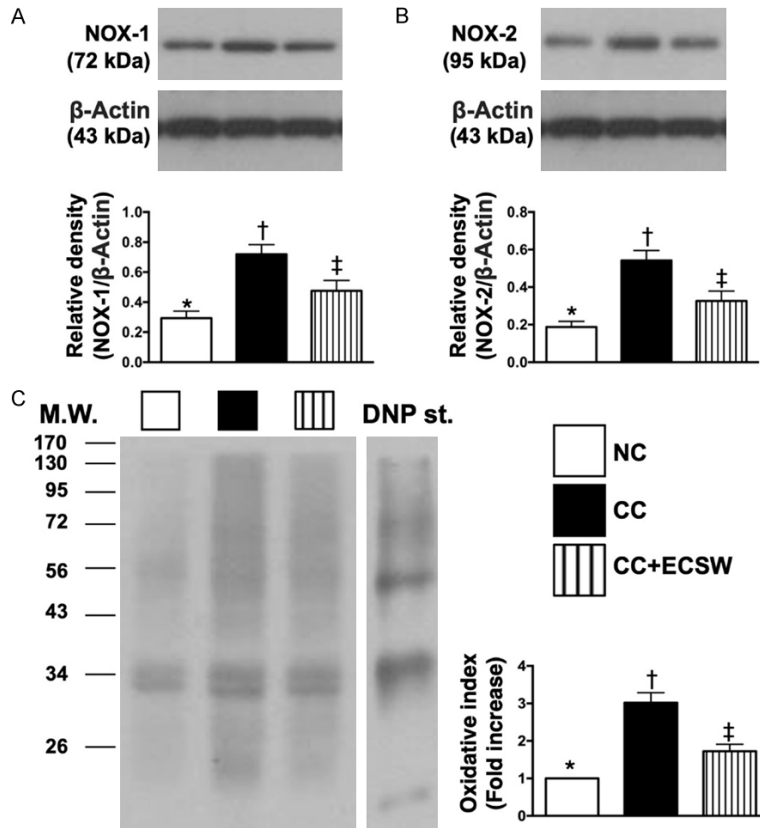
Figure 2. The protein levels of oxidative-stress biomarkers in urinary bladder by day 60 after CC induction. A. Protein expressions of NOX-1, * vs. other groups with different symbols (†, ‡), P < 0.001. B. Protein expression of NOX-2, * vs. other groups with different symbols (†, ‡), P < 0.0001. C. Oxidized protein expression in urinary bladder by day 60 after CC induction, * vs. other groups with different symbols (†, ‡), P < 0.0001. (Note: left and right lanes shown on the upper panel represent protein molecular weight marker and control oxidized molecular protein standard, respectively). M.W. = molecular weight; DNP = 1-3 dinitrophenylhydrazone. All statistical analyses were performed by one-way ANOVA, followed by Bonferroni multiple comparison post hoc test (n = 6 for each group). Symbols (*, †, ‡) indicate significance at the 0.05 level. NC = normal control; CC = chronic cystitis; ECSW = extracorporeal shock wave.

buffer [5% nonfat dry milk in T-TBS (TBS containing 0.05% Tween 20)] overnight. The membranes were incubated with the indicated primary antibodies [matrix metalloproteinase (MMP)-9 (1:1000, Abcam), tumor necrosis factor (TNF)-α (1:1000, Cell Signaling), phosphorylated (p)-nuclear factor (NF)-κB (1:600, Abcam), NOX-1 (1:1500, Sigma), NOX-2 (1:750, Sigma), TLR-4 (1:1000, Abcam), myeloid differentiation primary response 88 (MYD88) (1:1000, Abcam), Mal (1:1000, Abcam), tumor necrosis factor receptor associated factor (TRAF) (1:1000, Abcam), p-IκBα (1:1000, Cell Signaling), cleaved caspase 3 (1:1000, Cell Signaling), cleaved poly (ADP-ribose) polymerase (c-PARP) (1:1000, Cell Signaling), transforming growth factor (TGF)-β (1:500, Abcam), p-Smad3 (1:1000, Cell Signaling) and actin (1:10000, Chemicon)] for 1 hour at room temperature. Horseradish peroxidase-conjugated anti-rabbit immunoglobulin IgG (1:2000, Cell Signaling) was used as a secondary antibody for one-hour incubation at room temperature. Immunoreactive bands were visualized by enhanced chemiluminescence (ECL; Amersham Biosciences) and exposed to Biomax L film (Kodak). For the purpose of quantification, ECL signals were digitized using Labwork software (UVP).

Statistical analysis

Quantitative data are expressed as mean ± SD. Statistical analysis was adequately performed by ANOVA followed by Bonferroni multiple-comparison post hoc test. SAS statistical software for Windows version 8.2 (SAS institute, Cary, NC, USA) was utilized. A probability value < 0.05 was considered statistically significant.
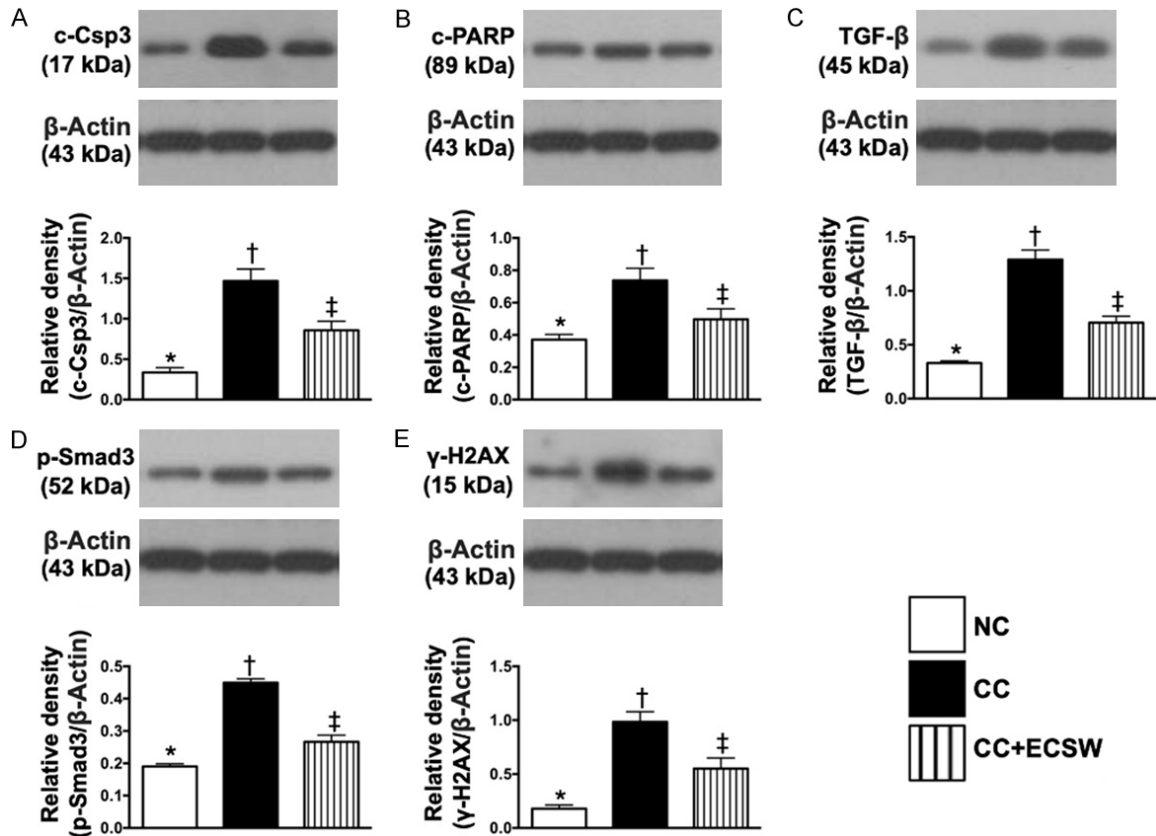
(11-25%), 3 (26-45%), 4 (46-75%), and 5 (≥ 76%).

Western blot analysis

The procedure and protocol for Western blot analysis were based on our previous reports (24, 26-33). Briefly, equal amounts (50 mg) of protein extracts were loaded and separated by SDS-PAGE using acrylamide gradients. After electrophoresis, the separated proteins were transferred electrophoretically to a polyvinylidene difluoride (PVDF) membrane (Amersham Biosciences). Nonspecific sites were blocked by incubation of the membrane in blocking

Figure 3. Protein expressions of apoptosis, fibrosis and DNA-damaged marker in urinary bladder by day 60 after CC induction. A. Protein expressions of cleaved caspase 3 (c-Csp3), * vs. other groups with different symbols (†, ‡), P < 0.0001. B. Protein expression of cleaved poly (ADP-ribose) polymerase (c-PARP), * vs. other groups with different symbols (†, ‡), P < 0.0001. C. Protein expression of transforming growth factor (TGF)-β, * vs. other groups with different symbols (†, ‡), P = 0.002. D. Protein expression of phosphorylated (p)-Smad3, * vs. other groups with different symbols (†, ‡), P < 0.0001. E. Protein expression of γ-H2AX, * vs. other groups with different symbols (†, ‡), P < 0.0001. All statistical analyses were performed by one-way ANOVA, followed by Bonferroni multiple comparison post hoc test (n = 6 for each group). Symbols (*, †, ‡) indicate significance at the 0.05 level. NC = normal control; CC = chronic cystitis; ECSW = extracorporeal shock wave.

Results

*Urodynamic study of bladder contraction, urine amount and ratio of urine protein to urine creatinine at day 60 after radiotherapy (**Figure 1**)*

By day 60, i.e., the end of study period, the urodynamic patterns showed that as compared with NC, significantly impaired detrusor contractility was identified in CC that was substantially reversed in CC animals after receiving ECSW treatment.

By the end of study period, the urine amount was significantly increased in CC than in NC and CC-ECSW, and significantly increased in CC-ECSW than in NC. However, the ratio of urine protein to urine creatinine was significant-ly reduced in CC and CC-ECSW than in NC, but it did not differ between the CC and CC-ECSW, suggesting that the urine bladder function was impaired by brachytherapy.

*Time courses of sporadic urine-routine examination (**Table 1**)*

Urine routine results showed that the occulted blood, proteinuria, glucose, nitrate, red blood cell, white blood cell, leukocyte, bacteria and cast formation in sporadic urine sample were found to be within the normal range among the three groups at day 0 prior to CC induction.

However, by day 28 after CC induction, the occulted blood, leukocyte, nitrite, white blo-
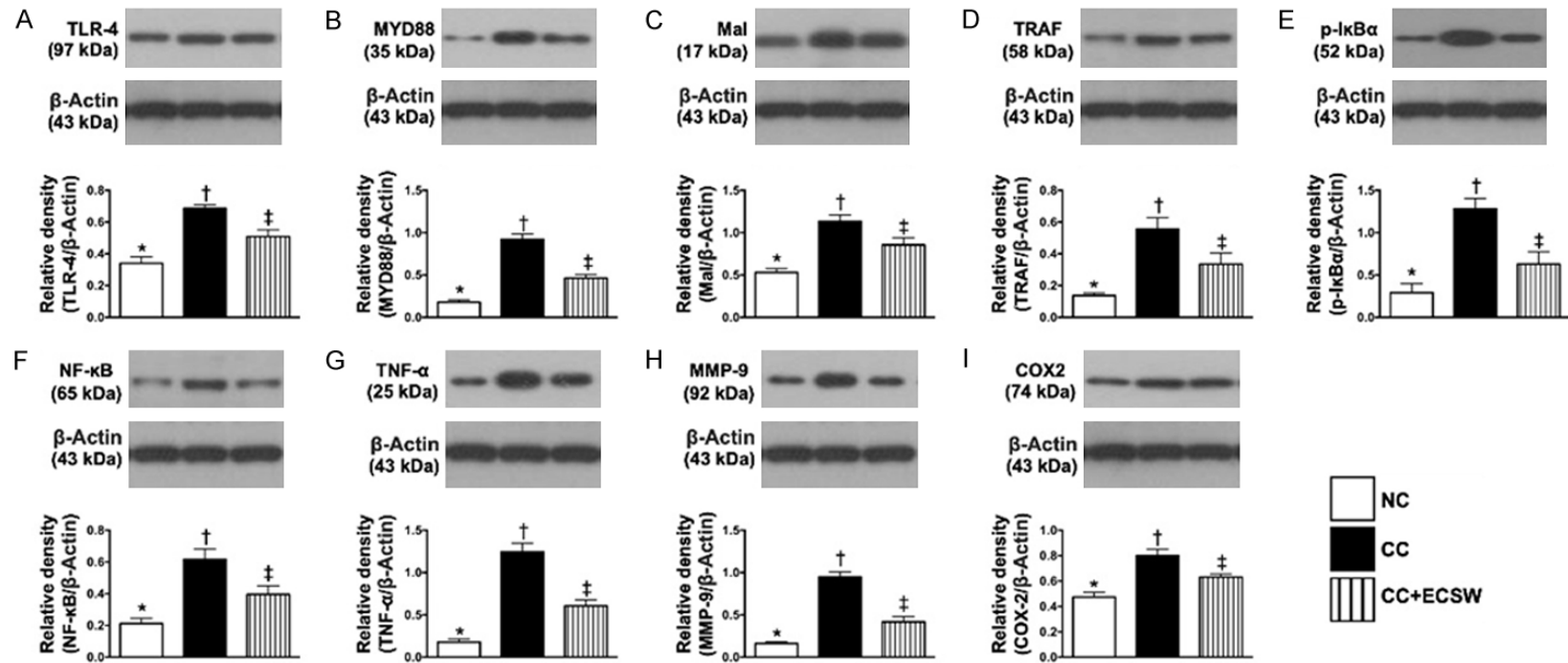
Figure 4. Protein expressions of up- and down-stream inflammatory signaling in urinary bladder by day 60 after CC induction. A. Protein expression of toll-like receptor (TLR)-4, * vs. other groups with different symbols (†, ‡), P < 0.0001. B. Protein expression of myeloid differentiation primary response 88 (MYD88), * vs. other groups with different symbols (†, ‡), P < 0.0001. C. Protein expression of Mal, * vs. other groups with different symbols (†, ‡), P < 0.0001. D. Protein expression of tumor necrosis factor (TNF) receptor associated factor (TRAF), * vs. other groups with different symbols (†, ‡), P < 0.001. E. Protein expression of phosphorylated (p)-IκBα, * vs. other groups with different symbols (†, ‡), P < 0.0001. F. Protein expression of p-NF-κB, * vs. other groups with different symbols (†, ‡), P < 0.0001. G. Protein expression of TNF-α, * vs. other groups with different symbols (†, ‡), P < 0.0001. H. Protein expression of matrix metalloproteinase (MMP)-9, * vs. other groups with different symbols (†, ‡), P < 0.0001. I. Protein expression of COX-2, * vs. other groups with different symbols (†, ‡), P < 0.0001. All statistical analyses were performed by one-way ANOVA, followed by Bonferroni multiple comparison post hoc test (n = 6 for each group). Symbols (*, †, ‡) indicate significance at the 0.05 level. NC = normal control; CC = chronic cystitis; ECSW = extracorporeal shock wave.
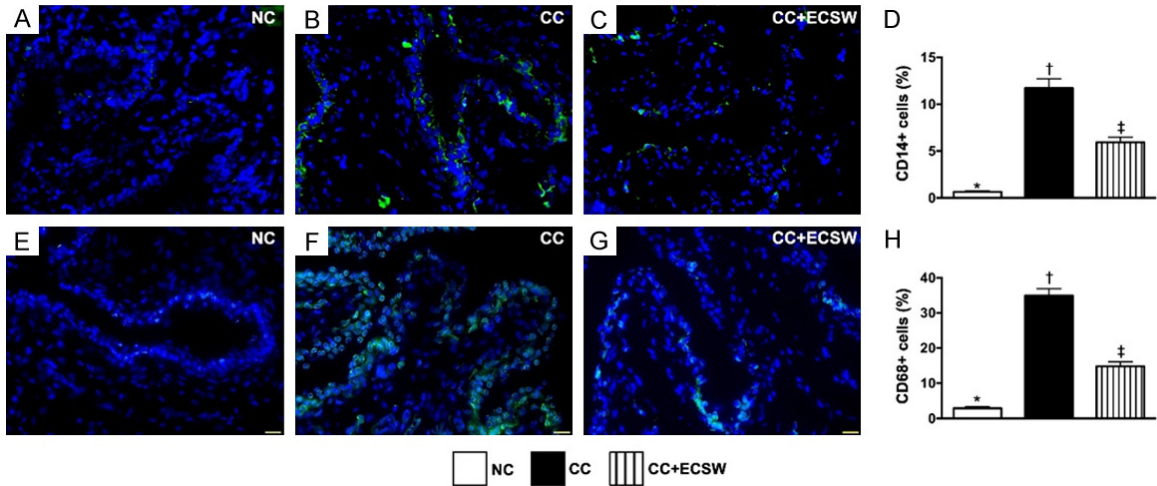
Figure 5. CD14 and CD68 inflammatory cell infiltrations in urinary bladder by day 60 after CC induction. A-C. Illustrating the immunofluorescent (IF) microscopic finding (400 ×) of CD14+ cells (green color). D. Analytical results of number of CD14+ cells, * vs. other groups with different symbols (†, ‡), P < 0.0001. E-G. Illustrating the IF microscopic finding (400x) of CD68+ cells (green color). H. Analytical results of number of CD68+ cells, * vs. other groups with different symbols (†, ‡), P < 0.0001. Scale bars in the right lower corner represent 20 μm. All statistical analyses were performed by one-way ANOVA, followed by Bonferroni multiple comparison post hoc test (n = 6 for each group). Symbols (*, †, ‡) indicate significance at the 0.05 level. NC = normal control; CC = chronic cystitis; ECSW = extracorporeal shock wave.
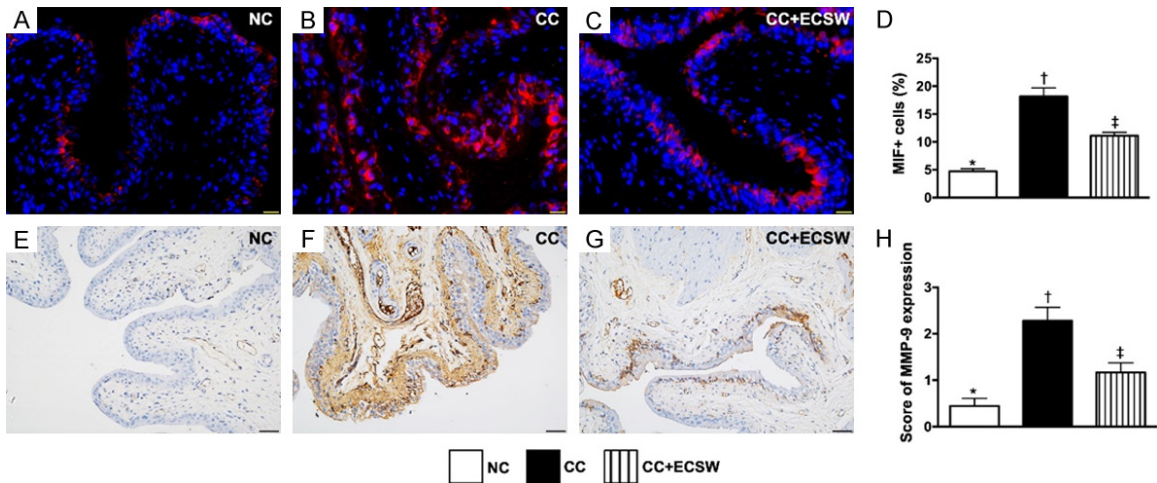

Figure 6. MIF and MMP-9 inflammatory cell infiltrations in urinary bladder by day 60 after CC induction. A-C. Illustrating the immunofluorescent microscopic finding (400 ×) for identification of macrophage migration inhibitory factor (MIF)+ cells (red color). D. Analytical result of number of MIF+ cells, * vs. other groups with different symbols (†, ‡), P < 0.0001. Scale bars in the right lower corner represent 20 μm. E-G. Illustrating the microscopic finding (200x) of immunohistochemical stain for identification of matrix metalloproteinase (MMP)-9 expression (gray color) in urinary bladder. H. Analytical results of MMP-9 expression, * vs. other groups with different symbols (†, ‡), P < 0.0001. Scale bars in the right lower corner represent 50 μm. All statistical analyses were performed by one-way ANOVA, followed by Bonferroni multiple comparison post hoc test (n = 6 for each group). Symbols (*, †, ‡) indicate significance at the 0.05 level. NC = normal control; CC = chronic cystitis; ECSW = extracorporeal shock wave.

od cell count and bacteria were significantly higher in CC than in NC and CC-ECSW, whereas only white blood cell count, nitrite and bacteria were significantly higher in CC-ECSW than in NC.

Furthermore, by day 60 after CC induction, nitrite, leukocyte, white blood cell count and bacteria were significantly higher in CC than in NC and CC-ECSW, but they showed no difference between the latter two groups.
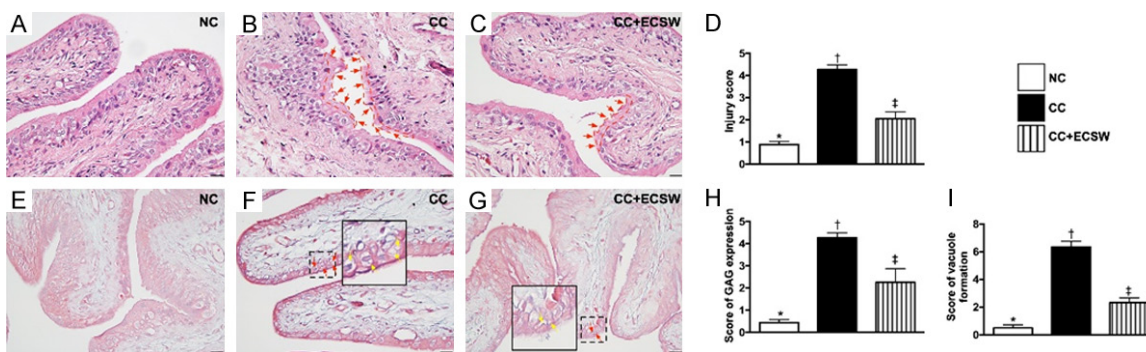
Figure 7. Histopathological findings of urinary bladder at day 60 after CC induction. (A-C) Illustrating the microscopic finding (200 ×) of H.E. stain for identification of injury of epithelial layer. The integrity of epithelial layer in CC was destroyed (B) (red arrows) as compared with NC (A). On the contrary, the integrity was notably preserved in CC after receiving ECSW therapy (C). (D) Analytical result of the injury score of epithelial layer by day 60 after CC induction, * vs. other groups with different symbols (†, ‡), P < 0.0001. (E-G) Illustrating the microscopic finding (200 ×) of immunohistochemical staining for identification of intensive expression of glycosaminoglycan (GAG) in epithelial layer of urinary bladder (pink color). (H) Quantitative analysis of GAG expression, * vs. other groups with different symbols (†, ‡), P < 0.0001. (I) Quantification of vacuole formation (yellow arrows) in epithelial layer by day 60 after CC induction, solid square was the manifestation of dot-line square for identification of vacuole formation (red arrows), * vs. other groups with different symbols (†, ‡), P < 0.0001. Scale bars in right lower corner represent 50 μm. All statistical analyses were performed by one-way ANOVA, followed by Bonferroni multiple comparison post hoc test (n = 6 for each group). Symbols (*, †, ‡) indicate significance at the 0.05 level. NC = normal control; CC = chronic cystitis; ECSW = extracorporeal shock wave.

*The protein level of oxidative-stress biomarkers in urinary bladder by day 60 after CC induction (**Figure 2** and Supplementary Figure 1)*

The protein expressions of NOX-1, NOX-2 and oxidized protein, three indicators of oxidative stress, were significantly increased in CC than in NC and CC-ECSW, and significantly increased in CC-ECSW than in NC.

*The protein expressions of apoptosis, fibrosis and DNA-damaged marker in urinary bladder by day 60 after CC induction (**Figure 3** and Supplementary Figure 2)*

The protein expressions of cleaved caspase 3 and cleaved PARP, two indicators of apoptosis, and protein expressions of TGF-β and Smad3, two indicators of fibrosis, were significantly higher in CC than in NC and CC-ECSW, and significantly higher in CC-ECSW than in NC. Additionally, the protein expression of γ-H2AX, an indicator of DNA-damaged marker, displayed an identical pattern of apoptosis among the three groups.

*The protein expressions of up- and down-stream inflammatory signaling in urinary bladder by day 60 after CC induction (**Figure 4** and Supplementary Figure 3)*

The protein expressions of TLR-4, MYD88, Mal, TRAF6, p-IκBα, p-NF-κB, TNF-α, MMP-9, and COX-2, eight inflammatory up- and down-stream inflammatory signaling biomarkers, were significantly upregulated in CC than in NC and CC-ECSW and significantly upregulated in CC-ECSW than in NC.

*Inflammatory cell infiltrations and histopathological findings of urinary bladder by day 60 after CC induction (**Figures 5**-**7**)*

The cellular expressions of CD14 and CD68, two indices of inflammation, were significantly higher in CC than in NC and CC-ECSW, and significantly higher in CC-ECSW than in NC (**Figure 5**).

Additionally, the cellular expressions of MIF and MMP-9, another two indices of inflammation, exhibited identical pattern of CD14 among the three groups (**Figure 6**).

Furthermore, the H.E. stain displayed that the injury score of epithelial layer was significantly increased in the CC than that in NC and CC-ECSW, and significantly increased in the CC-ECSW group than that in NC group. Moreover, IHC staining exhibited that the expression of GAG in the epithelial layer of the bladder, an indicator of disruption of the bladder mucosa surface layer, displayed a similar pattern compared to that of injury score of epithelial layer among the three groups. Besides,
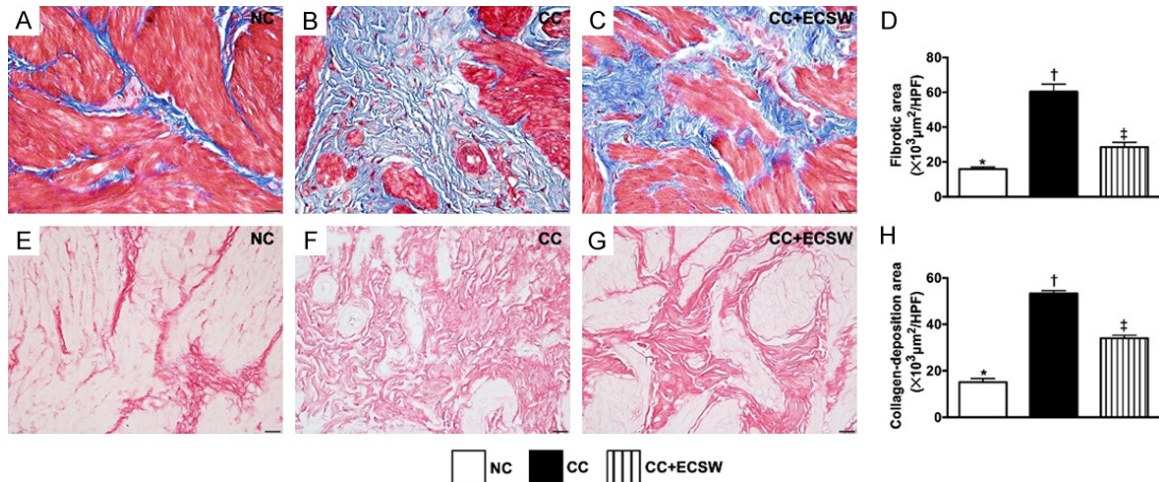
Figure 8. Fibrotic and collagen-deposition areas in urinary bladder by day 60 after CC induction. A-C. Illustrating the microscopic finding (400 ×) of Masson's trichrome stain for identification of fibrosis (blue color). D. Analytical result of fibrotic area, * vs. other groups with different symbols (†, ‡), P < 0.0001. E-G. Illustrating the microscopic finding (400 ×) of Sirius red stain for identification of collagen deposition expression (pink color). H. Analytical result of collagen-deposition area, * vs. other groups with different symbols (†, ‡), P < 0.0001. Scale bars in right lower corner represent 20 μm. All statistical analyses were performed by one-way ANOVA, followed by Bonferroni multiple comparison post hoc test (n = 6 for each group). Symbols (*, †, ‡) indicate significance at the 0.05 level. NC = normal control; CC = chronic cystitis; ECSW = extracorporeal shock wave.

the formation of vacuoles in epithelial layer also showed a pattern identical to that of injury score of epithelial layer among the three groups (**Figure 7**).

*Fibrotic and collagen-deposition areas in urinary bladder by day 60 after CC induction (**Figure 8**)*

The Masson's trichrome stain demonstrated that the fibrotic area was significantly increased in CC than in NC and CC-ECSW, and significantly increased in CC-ECSW than in NC. Additionally, the Sirius red stain showed that the collagen-deposition area expressed a similar pattern of fibrosis among the three groups.

*T-cell expressions in urinary bladder by day 60 after CC induction (**Figure 9**)*

The cellular expressions of CD4 and CD8, two indicators of immune cells, were significantly higher in CC than in NC and CC-ECSW, and significantly higher in CC-ESCW than in NC.

*Expressions of cytokeratin (CK) in urinary bladder by day 60 after CC induction (**Figure 10**)*

The IHC staining showed that the expressions of CK17+ and CK-18+ cells, two indicators of

keratin-phenotype epithelial cells, were significantly higher in the CC than in NC and CC-ECSW, and significantly higher in CC-ECSW than in NC.

Discussion

This study which investigated the optimal dosage and long-term effect of ECSW therapy on protecting the urinary bladder against the radiation-induced CC yielded several striking preclinical implications. First, the optimal dose of radiation was 450 cGy twice at a time interval of 4 h in rodent CC model. Second, the long-term effect of ECSW on CC was promising. Third, the results of this study demonstrated that inflammatory signaling pathway played an essential role on radiation-induced CC that was effectively supressed by regularly intermittent applications of ECSW therapy.

Currently, despite an array of feasible modalities for the treatment of radiation-induced CC [11-18], there is still lacking an effective method for this disease entity, highlighting that the treatment of radiation-induced CC in patients with advanced urogenital organ malignancy remains a formidable challenge. Based on the results of our recent study [31], we modified the time points of ECSW application (i.e., once
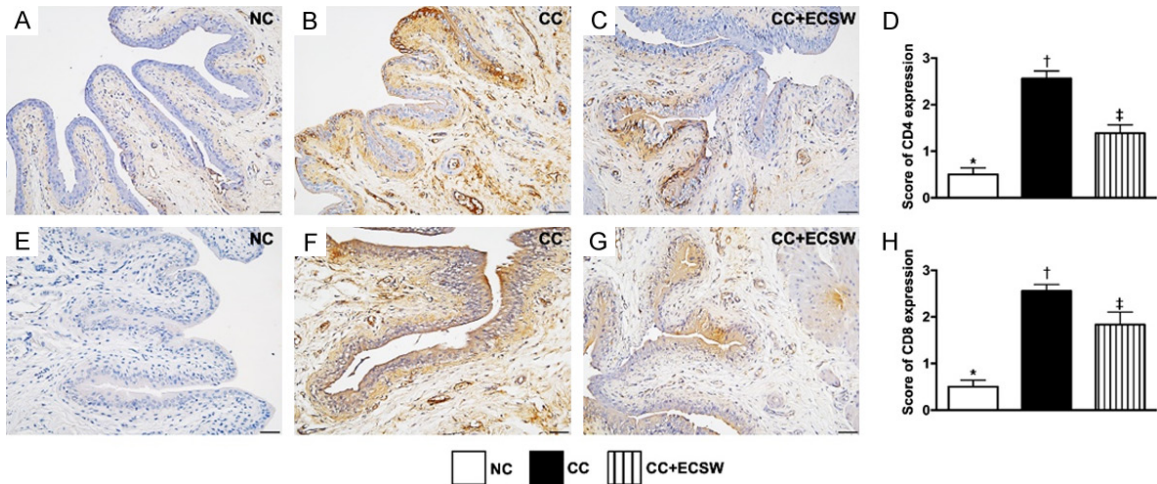
Figure 9. Immune cell expressions in urinary bladder by day 60 after CC induction. A-C. Illustrating microscopic finding (200 ×) of immunohistochemical (IHC) stain for identification of cellular expression of CD4 (gray color). D. Analytical result of CD4 expression, * vs. other groups with different symbols (†, ‡), P < 0.0001. E-G. Illustrating IHC microscopic finding (200 ×) for identification of cellular expression of CD8 (gray color). H. Analytical result of CD8 expression, * vs. other groups with different symbols (†, ‡), P < 0.0001. Scale bars in right lower corner represent 50 μm. All statistical analyses were performed by one-way ANOVA, followed by Bonferroni multiple comparison post hoc test (n = 6 for each group). Symbols (*, †, ‡) indicate significance at the 0.05 level. NC = normal control; CC = chronic cystitis; ECSW = extracorporeal shock wave.
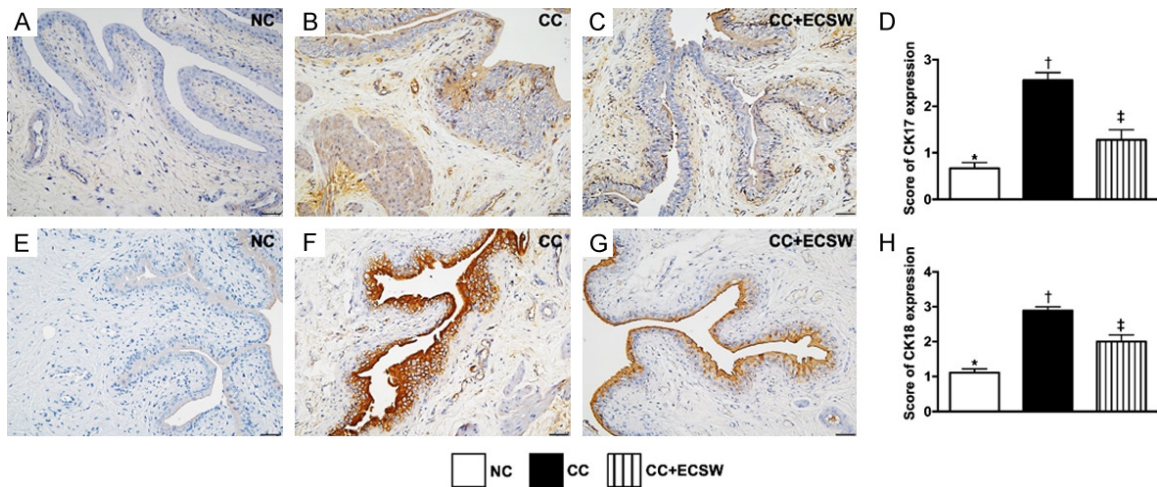

Figure 10. Expressions of cytokeratin (CK)17+ and CK18+ cells in urinary bladder at day 60 after CC induction. A-C. Illustrating microscopic finding (400 ×) of immunohistochemical (IHC) staining for identification of the expression of CK17 (gray color) in urinary bladder by day 60 after CC induction. D. Analytical result of CK17 expression by day 60 after CC induction, * vs. other groups with different symbols (†, ‡), P < 0.0001. E-G. Illustrating IHC microscopic finding (400 ×) for identification of the expression of CK18 (brown color) in urinary bladder by day 60 after CC induction. H. Analytical result of CK18 expression by day 60 after CC induction, * vs. other groups with different symbols (†, ‡), P < 0.0001. Scale bars in right lower corner represent 20 μm. All statistical analyses were performed by one-way ANOVA, followed by Bonferroni multiple comparison post hoc test (n = 6 for each group). Symbols (*, †, ‡) indicate significance at the 0.05 level. NC = normal control; CC = chronic cystitis; ECSW = extracorporeal shock wave.

every 3 days, named "regularly intermittent administration") for those radiotherapy-induced CC animals in the present study to determine the long-term impact of this innovative therapy. The most important finding in the present study was that the urodynamic study showed, as compared with the CC animals, the detrusor contractility was significantly preserved in CC-ECSW animals. Additionally, the urine analyses demonstrated that white blood cell count,
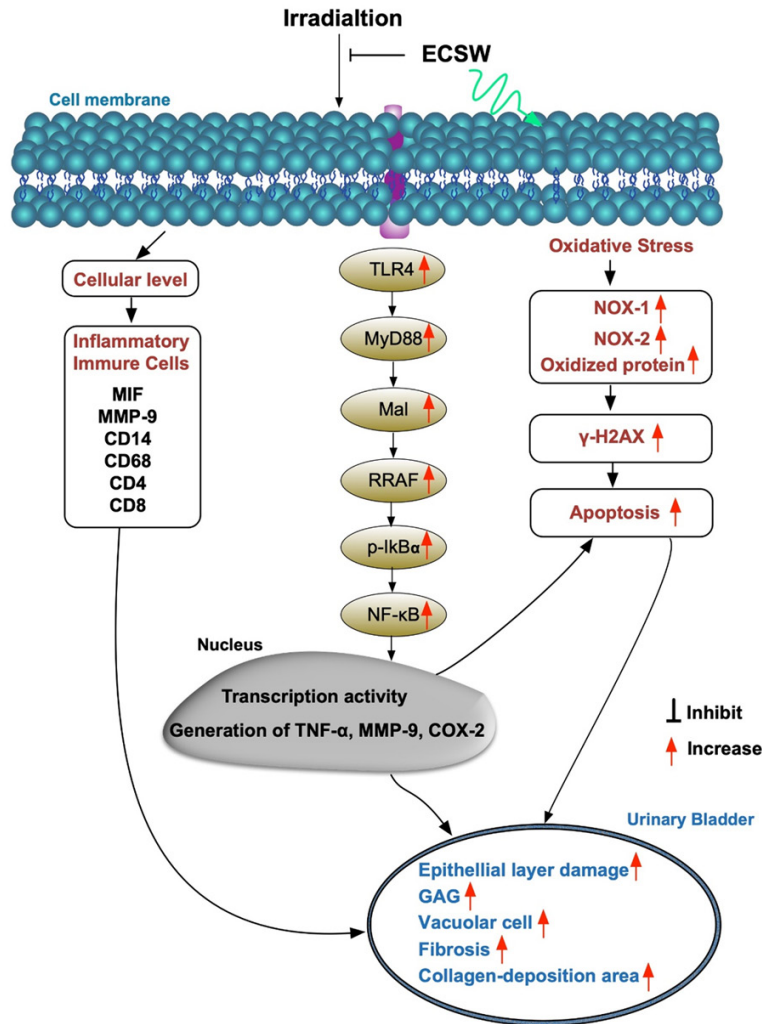
Figure 11. Schematically proposed mechanism of radiation-induced urinary bladder chronic cystitis based on the results of the present study. MMP = macrophage; MIF macrophage migratory inhibitor; TGF-β = transforming growth factor; ECSW = extracorporeal shock wave; TLR = toll-like receptor; MYD88 = myeloid differentiation primary response 88; TRAF = tumor necrosis factor (TNF) receptor associated factor; GAG = glycosaminoglycan.

need of thorough investigation in this area. A principal finding in the present study was that the up- and downstream inflammatory signaling pathways were clearly identified to participate in the radiotherapy-induced CC (refer to **Figure 11**). Additionally, not only the protein levels but also the cellular levels of inflammatory biomarkers and immune cells were identified to substantially infiltrate into the urinary bladder of CC animals. Furthermore, the muscular damage score (i.e., indicator of tissue necrosis) demonstrated through H.E. stain and the fibrosis/collagen deposition identified by IHC statin were remarkably increased in those of CC animals. Intriguingly, a strong association between inflammatory reaction and tissue necrosis/fibrosis and organ damage has been well recognized in the previous studies [23, 25-30, 32]. Our findings, in addition to strengthening the findings of previous studies [23, 25-30, 32], clearly delineate the strong correlation among the inflammation, tissue/organ damage and radiotherapy. Of particular important finding in the present study was that regularly intermittent application of ECSW significantly preserved the architectural integrity and the function of urinary bladder in setting of CC that was soundly proved mainly through effectively ameliorating these molecular-cellular perturbations.

Preponderance of evidence has displayed that the generations of oxidative stress, cellular apoptosis and DNA damage are commonly found in all causal etiologies of organ damage [23, 25-29, 32]. These pathological parameters were also identified in our previous study of CC animals [30]. The essential finding in the present study was that the oxidative-stress, apop-

bacteria and occult blood were significantly increased in CC group than in NC group, and remarkably reversed in CC animals after receiving regularly intermittent ECSW therapy (**Table 1**). Our findings, in addition to extending the findings of our recent study [30], highlight that this innovative therapy should be considered for those of CC patients, especially when they are refractory to conventional therapy.

The underlying mechanisms of radiotherapy-induced CC in cellular-molecular levels have not often been reported [19, 30], leaving an urgent

totic and DNA-damaged and cytokeratin (i.e., CK17, CK18) biomarkers were extremely higher in CC animals. Our findings were consistent with the findings of previous studies [23, 25-30, 32]. Of distinctive finding was that these parameters were markedly reduced in CC animals treated by ECSW, once again explained why the architecture and function of urinary bladder were preserved in CC animals after receiving ECSW.

Study limitation

This study has limitations. Frist, this study did not test the energy dose of ECSW in stepwise manner. Accordingly, we did not provide the optimal dose of ECSW as a reference for clinical application of this therapy for CC patients. Second, based on the previous reports [19, 30], an investigation of underlying mechanisms in setting of radiation-induced CC in rat focused more on the inflammatory signaling pathway in the present study (**Figure 11**). This may raise the concern of bias due to incomplete investigation. In fact, the signaling mechanism of radiation-induced CC may be more complex and comprises multiple signaling pathways.

In conclusion, regularly intermittent application of low-energy ECSW therapy effectively protects the architectural and functional integrities of urinary bladder in CC rats.

Acknowledgements

Disclosure of conflict of interest

None.

Address correspondence to: Dr. Eng-Yen Huang, Department of Radiation Oncology, Kaohsiung Chang Gung Memorial Hospital, Chang Gung University College of Medicine, Kaohsiung, No. 123, Dapi Road, Niaosong District, Kaohsiung, Taiwan. Tel: +86-7-7317123; Fax: +86-7-7322813; E-mail: huangengyen@gmail.com; Hon-Kan Yip, Division of Cardiology, Department of Internal Medicine, Kaohsiung Chang Gung Memorial Hospital, Chang Gung University College of Medicine, 123, Dapi Road, Niaosung District, Kaohsiung 83301, Taiwan. Tel: +86-7-7317123; Fax: +86-7-7322402; E-mail: han.gung@msa.hinet.net

References

[1] Aghili M, Andalib B, Karimi Moghaddam Z, Maddah Safaie A, Amoozgar Hashemi F and Mousavi Darzikolaie N. Concurrent chemo-radiobrachytherapy with cisplatin and medium dose rate intra- cavitary brachytherapy for locally advanced uterine cervical cancer. Asian Pac J Cancer Prev 2018; 19: 2745-2750.

[2] Liu P, Tong L, Huo B, Dai D, Liu W, Wang K, Wang Y, Guo Z and Ni H. CT-guided (125)I brachytherapy for recurrent ovarian cancer. Oncotarget 2017; 8: 59766-59776.

[3] Raleigh DR, Seymour ZA, Tomlin B, Theodosopoulos PV, Berger MS, Aghi MK, Geneser SE, Krishnamurthy D, Fogh SE, Sneed PK and McDermott MW. Resection and brain brachytherapy with permanent iodine-125 sources for brain metastasis. J Neurosurg 2017; 126: 1749-1755.

[4] Stewart A, Parashar B, Patel M, O'Farrell D, Biagioli M, Devlin P and Mutyala S. American brachytherapy society consensus guidelines for thoracic brachytherapy for lung cancer. Brachytherapy 2016; 15: 1-11.

[5] Zaorsky NG, Davis BJ, Nguyen PL, Showalter TN, Hoskin PJ, Yoshioka Y, Morton GC and Horwitz EM. The evolution of brachytherapy for prostate cancer. Nat Rev Urol 2017; 14: 415-439.

[6] Alesawi AM, El-Hakim A, Zorn KC and Saad F. Radiation-induced hemorrhagic cystitis. Curr Opin Support Palliat Care 2014; 8: 235-240.

[7] Grellety T, Houede N, Hoepffner JL, Rivière J, Mérino C, Lieutenant V, Gross-Goupil M, Richaud P, Dupin C, Sargos P and Roubaud G. Hemorrhagic cystitis in patients treated with cabazitaxel: a radiation recall syndrome? Ann Oncol 2014; 25: 1248-1249.

[8] Mendenhall WM, Henderson RH, Costa JA, Hoppe BS, Dagan R, Bryant CM, Nichols RC, Williams CR, Harris SE and Mendenhall NP. Hemorrhagic radiation cystitis. Am J Clin Oncol 2015; 38: 331-336.

[9] Payne H, Adamson A, Bahl A, Borwell J, Dodds D, Heath C, Huddart R, McMenemin R, Patel P, Peters JL and Thompson A. Chemical- and radiation-induced haemorrhagic cystitis: current treatments and challenges. BJU Int 2013; 112: 885-897.

[10] Viswanathan AN, Lee LJ, Eswara JR, Horowitz NS, Konstantinopoulos PA, Mirabeau-Beale KL, Rose BS, von Keudell AG and Wo JY. Complications of pelvic radiation in patients treated for gynecologic malignancies. Cancer 2014; 120: 3870-3883.

[11] Bonfili P, Franzese P, Marampon F, La Verghetta ME, Parente S, Cerasani M, Di Genova D, Mancini M, Vittorini F, Gravina GL, Ruggieri V, Di Staso M, Popov VM, Tombolini V and Di Cesare E. Intravesical instillations with polydeoxyribonucleotides reduce symptoms of radiation-induced cystitis in patients treated with radiotherapy for pelvic cancer: a pilot study. Support Care Cancer 2014; 22: 1155-1159.

[12] Linder BJ, Tarrell RF and Boorjian SA. Cystectomy for refractory hemorrhagic cystitis: contemporary etiology, presentation and outcomes. J Urol 2014; 192: 1687-1692.

[13] Oliai C, Fisher B, Jani A, Wong M, Poli J, Brady LW and Komarnicky LT. Hyperbaric oxygen therapy for radiation-induced cystitis and proctitis. Int J Radiat Oncol Biol Phys 2012; 84: 733-740.

[14] Rajaganapathy BR, Jayabalan N, Tyagi P, Kaufman J and Chancellor MB. Advances in therapeutic development for radiation cystitis. Low Urin Tract Symptoms 2014; 6: 1-10.

[15] Shao Y, Lu GL and Shen ZJ. Comparison of intravesical hyaluronic acid instillation and hyperbaric oxygen in the treatment of radiation-induced hemorrhagic cystitis. BJU Int 2012; 109: 691-694.

[16] Talab SS, McDougal WS, Wu CL and Tabatabaei S. Mucosa-sparing, KTP laser coagulation of submucosal telangiectatic vessels in patients with radiation-induced cystitis: a novel approach. Urology 2014; 84: 478-483.

[17] Vilar DG, Fadrique GG, Martin IJ, Aguado JM, Perelló CG, Argente VG, Sanz MB and Gómez JG. Hyperbaric oxygen therapy for the management of hemorrhagic radio-induced cystitis. Arch Esp Urol 2011; 64: 869-874.

[18] Sommariva ML, Lazzeri M, Abrate A, et al. Intravesical hyaluronic acid and chondroitin sulphate improve symptoms and quality of life in patients with late radiation tissue cystitis: an investigative pilot study. Eur J Inflamm 2014; 12: 177-185.

[19] Browne C, Davis NF, Mac Craith E, Lennon GM, Mulvin DW, Quinlan DM, Mc Vey GP and Galvin DJ. A Narrative review on the pathophysiology and management for radiation cystitis. Adv Urol 2015; 2015: 346812.

[20] Marks LB, Carroll PR, Dugan TC and Anscher MS. The response of the urinary bladder, urethra, and ureter to radiation and chemotherapy. Int J Radiat Oncol Biol Phys 1995; 31: 1257-1280.

[21] Pavlidakey PG and MacLennan GT. Radiation cystitis. J Urol 2009; 182: 1172-1173.

[22] Rapariz-Gonzalez M, Castro-Diaz D and Mejia-Rendon D; EURCIS. Evaluation of the impact of the urinary symptoms on quality of life of patients with painful bladder syndrome/chronic pelvic pain and radiation cystitis: EURCIS study. Actas Urol Esp 2014; 38: 224-231.

[23] Chen YT, Yang CC, Sun CK, Chiang HJ, Chen YL, Sung PH, Zhen YY, Huang TH, Chang CL, Chen HH, Chang HW and Yip HK. Extracorporeal shock wave therapy ameliorates cyclophosphamide-induced rat acute interstitial cystitis though inhibiting inflammation and oxidative stress-in vitro and in vivo experiment studies. Am J Transl Res 2014; 6: 631-648.

[24] Wang CJ, Wang FS, Yang KD, Weng LH and Ko JY. Long-term results of extracorporeal shockwave treatment for plantar fasciitis. Am J Sports Med 2006; 34: 592-596.

[25] Chen KH, Yang CH, Wallace CG, Lin CR, Liu CK, Yin TC, Huang TH, Chen YL, Sun CK and Yip HK. Combination therapy with extracorporeal shock wave and melatonin markedly attenuated neuropathic pain in rat. Am J Transl Res 2017; 9: 4593-4606.

[26] Chen YL, Chen KH, Yin TC, Huang TH, Yuen CM, Chung SY, Sung PH, Tong MS, Chen CH, Chang HW, Lin KC, Ko SF and Yip HK. Extracorporeal shock wave therapy effectively prevented diabetic neuropathy. Am J Transl Res 2015; 7: 2543-2560.

[27] Fu M, Sun CK, Lin YC, Wang CJ, Wu CJ, Ko SF, Chua S, Sheu JJ, Chiang CH, Shao PL, Leu S and Yip HK. Extracorporeal shock wave therapy reverses ischemia-related left ventricular dysfunction and remodeling: molecular-cellular and functional assessment. PLoS One 2011; 6: e24342.

[28] Sheu JJ, Lee FY, Yuen CM, Chen YL, Huang TH, Chua S, Chen YL, Chen CH, Chai HT, Sung PH, Chang HW, Sun CK and Yip HK. Combined therapy with shock wave and autologous bone marrow-derived mesenchymal stem cells alleviates left ventricular dysfunction and remodeling through inhibiting inflammatory stimuli, oxidative stress & enhancing angiogenesis in a swine myocardial infarction model. Int J Cardiol 2015; 193: 69-83.

[29] Yeh KH, Sheu JJ, Lin YC, Sun CK, Chang LT, Kao YH, Yen CH, Shao PL, Tsai TH, Chen YL, Chua S, Leu S and Yip HK. Benefit of combined extracorporeal shock wave and bone marrow-derived endothelial progenitor cells in protection against critical limb ischemia in rats. Crit Care Med 2012; 40: 169-177.

[30] Chen YT, Chen KH, Sung PH, Yang CC, Cheng BC, Chen CH, Chang CL, Sheu JJ, Lee FY, Shao PL, Sun CK and Yip HK. Extracorporeal shock wave markedly alleviates radiation-induced chronic cystitis in rat. Am J Transl Res 2018; 10: 1036-1052.

[31] Lee FY, Zhen YY, Yuen CM, Fan R, Chen YT, Sheu JJ, Chen YL, Wang CJ, Sun CK and Yip HK. The mTOR-FAK mechanotransduction signaling axis for focal adhesion maturation and cell proliferation. Am J Transl Res 2017; 9: 1603-1617.

[32] Shao PL, Chiu CC, Yuen CM, Chua S, Chang LT, Sheu JJ, Sun CK, Wu CJ, Wang CJ and Yip HK. Shock wave therapy effectively attenuates inflammation in rat carotid artery following endothelial denudation by balloon catheter. Cardiology 2010; 115: 130-144.
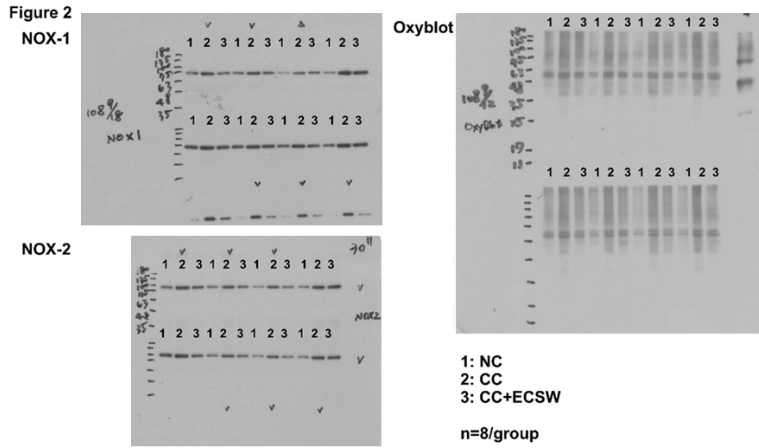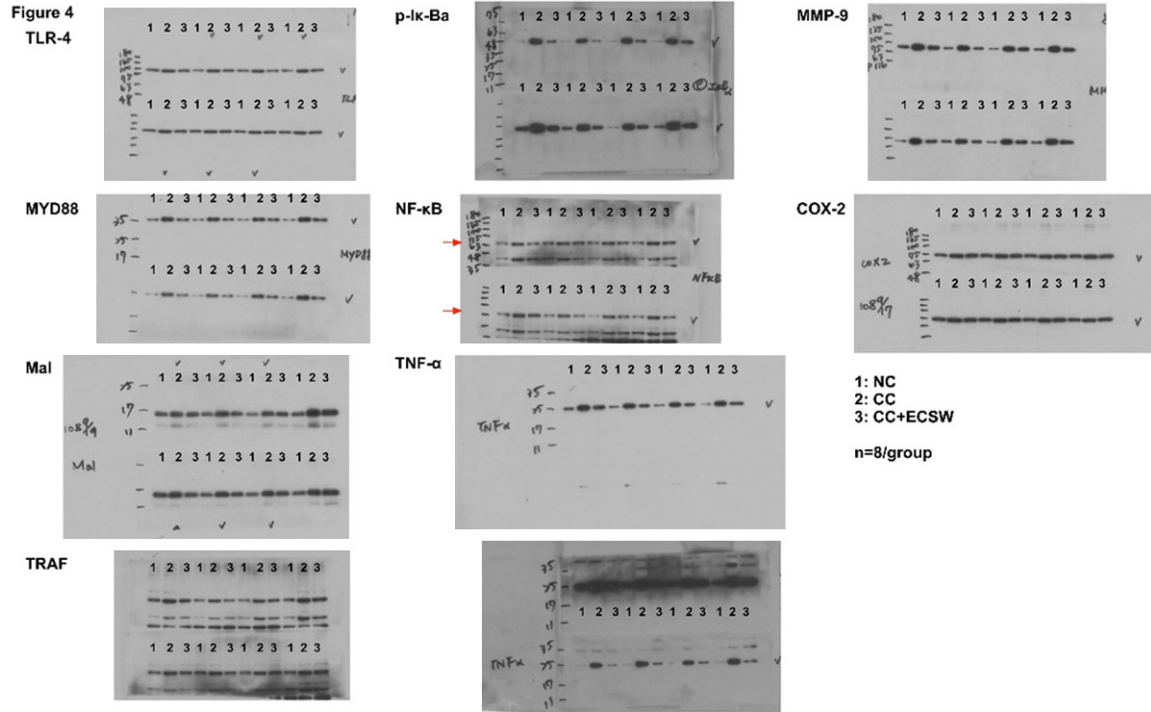
Supplementary Figure 1. Illustrating the raw materials of Western blot for identification of the expression of oxidative stress biomarkers.
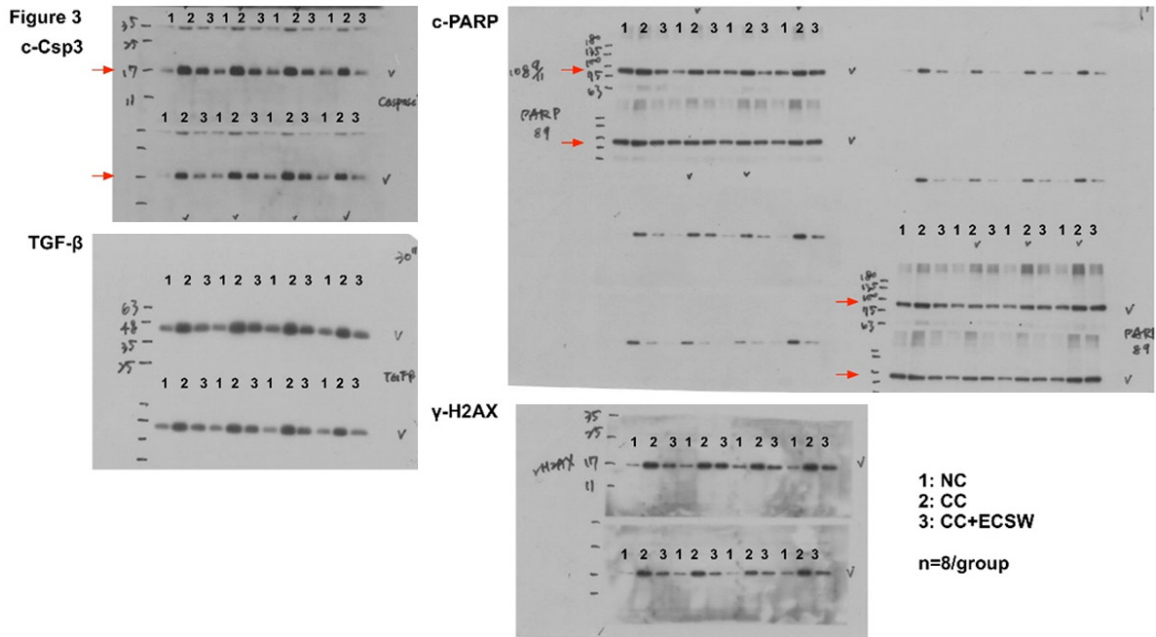
Supplementary Figure 2. Illustrating the raw materials of Western blot for identification of the expression of apoptotic, fibrotic and DNA-damaged biomarkers.

1

Supplementary Figure 3. Illustrating the raw material of Western blot for identification of the expression of inflammatory signaling pathway.